

## Supporting Information

### Structure investigation of nanohybrid PDMA/silica hydrogels at rest and under uniaxial deformation.

Séverine Rose<sup>1</sup>, Alba Marcellan<sup>1</sup>, Tetsuharu Narita<sup>1</sup>, François Boué<sup>2</sup>, Fabrice Cousin<sup>2</sup> and Dominique Hourdet<sup>1\*</sup>

<sup>1</sup>ESPCI / Sorbonne Universités, UPMC Univ Paris 06 / CNRS, UMR 7615, SIMM, 10 rue Vauquelin, F-75005, Paris, France

<sup>2</sup>Laboratoire Léon Brillouin, CEA-CNRS, Saclay 91191 Gif-sur-Yvette Cedex, France

### Small Angle Neutron Scattering (SANS)

#### Experimental part

In order to investigate the contribution of both organic and inorganic components within hybrid hydrogels by SANS, contrast matching has been carried out using suitable H<sub>2</sub>O/D<sub>2</sub>O ratios. Taking into account the scattering length densities of H<sub>2</sub>O ( $\rho_{\text{H}_2\text{O}} = -0.56 \cdot 10^{-6} \text{ \AA}^{-2}$ ), PDMA ( $\rho_{\text{PDMA}} = 0.936 \cdot 10^{-6} \text{ \AA}^{-2}$ ), silica ( $\rho_{\text{f}} = 3.48 \cdot 10^{-6} \text{ \AA}^{-2}$ ) and D<sub>2</sub>O ( $\rho_{\text{D}_2\text{O}} = 6.41 \cdot 10^{-6} \text{ \AA}^{-2}$ ), the contrast matching of PDMA and silica can be achieved with the following volume ratios:

- 1) H<sub>2</sub>O/D<sub>2</sub>O = 0.79/0.21, named “solvent p” for matching the PDMA network (p=polymer),
- 2) H<sub>2</sub>O/D<sub>2</sub>O = 0.42/0.58, named “solvent f” for matching the silica nanoparticles (f=filler).

For that purpose, hybrid hydrogels were specially prepared, following the same general procedure, in three different aqueous environments: solvent p, solvent f and pure H<sub>2</sub>O. For hybrid hydrogels with high amounts of D<sub>2</sub>O, Ludox-TM50 was initially dialysed during two weeks in control D<sub>2</sub>O environment in order to get a stable and concentrated dispersion of silica in D<sub>2</sub>O (around 40 wt%), with pH  $\cong$  9 (pH = 8.6 as measured in D<sub>2</sub>O) and a conductivity of 4.9 mS/cm.

In order to perform SANS experiments on gel samples under controlled deformation and environment, a special cell has been designed in collaboration with the Laboratoire Léon Brillouin. The main specifications of the cell (see **Figure S1**), which is inserted in the automatic sample changer of the PAXY spectrometer, are the following:

- an efficient fixation setup for the gel sample that prevents sliding,
- an accurate control in situ of the sample elongation with micrometric screws,
- a tight fit cell with a fine control of the environment, such as temperature, solvent or humidity,
- quartz windows, tightly closed and transparent for neutrons, with a sufficient diameter for the neutrons beam (about 7.3 mm).

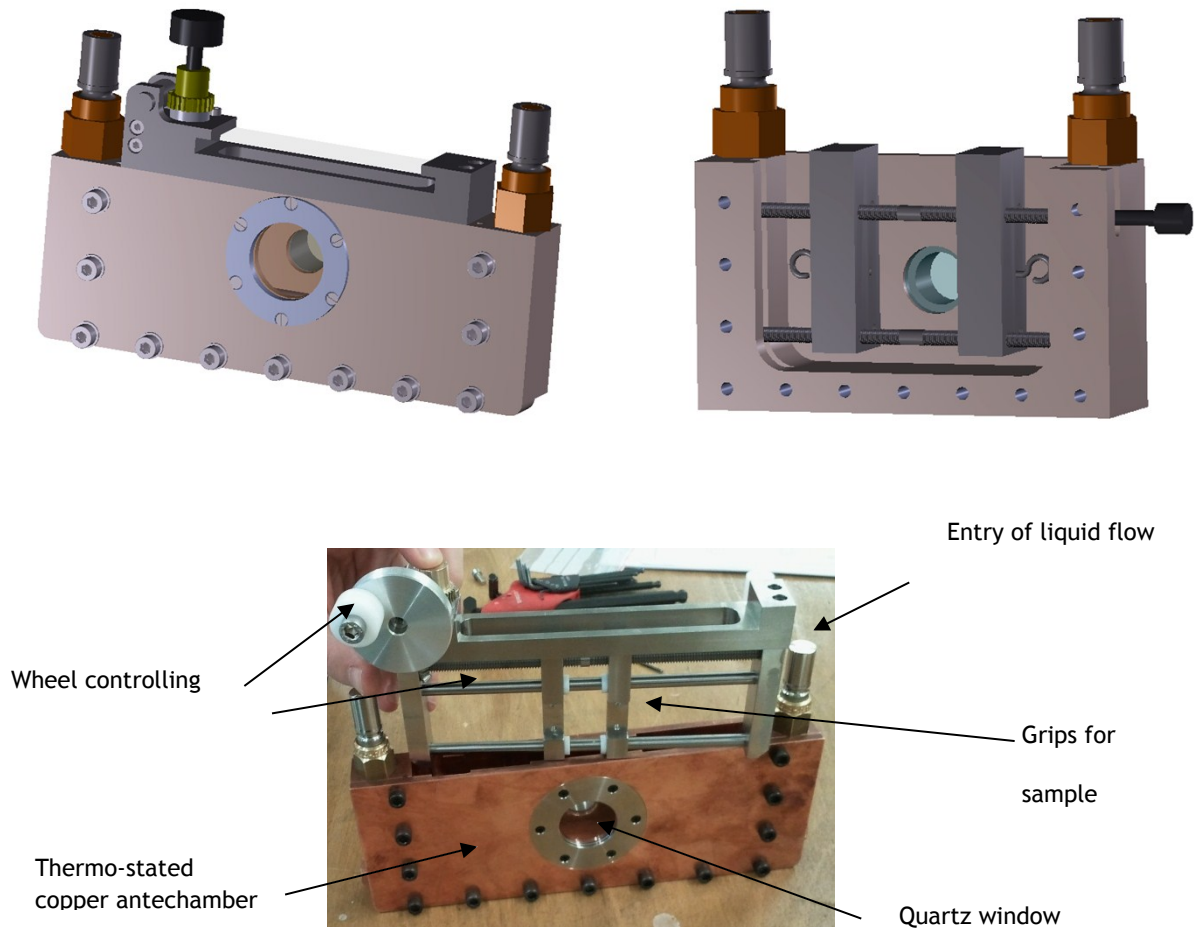


**Figure S1:** Up: Schematic representations of the 2D SANS device, with top left: the entire device, and top right: an internal view. Down: picture of the experimental device with legends.

In the case of hybrid hydrogels containing large amounts of water, a long stay in air induces drying that modifies the network properties (concentration, elastic modulus, etc...). This problem becomes critical with anisotropic analyses (longer acquisition times) performed on gel samples submitted to successive deformation states which could last for hours. For that reason, all anisotropic experiments on gel samples in their preparation state were carried out in immersed conditions; the cell chamber being filled with a fluorinated oil highly transparent for neutrons (perfluorodecalin). No interaction between hybrid hydrogels and fluorinated oil was observed in these conditions and hydrogels remained stable with time for hours, even days. In 2D SANS experiments, the incident neutron flux recorded on a two dimensional detector built up with 15500 cells of  $25 \text{ mm}^2$ , is directly transformed into a 2D image with a colour code. After sector averaging, the data can be quantitatively analyzed in terms of diffusion pattern.

### SANS analysis of dilute dispersion of Ludox TM-50

In dilute condition, when interactions between particles are negligible,  $S(q)=1$  over the whole range of  $q$  and  $I_{cor}(q)$  is equal to the form factor. An example is given in **Figure S2** with a dilute dispersion of Ludox TM50 (1 wt%) along with the fit obtained from the polydisperse sphere model. Even if the reduced scattering intensity, equal in these conditions to the form factor, is very noisy at large  $q$  after subtraction of the solvent, this first set of data allows a good assessment of the particle size; their volume being extrapolated at  $q \rightarrow 0$ :  $I_{cor}(0) = P(0) = V_f \cong 10^7 \text{ \AA}^3$ . The best fitting is obtained with a particle radius  $R_f = 132 \text{ \AA}$  and a standard deviation  $\sigma = 15 \text{ \AA}$ . These results are in good agreement with those obtained from other techniques, either in the dry state by SEM ( $R_f = 140\text{-}150 \text{ \AA}$  **Figure S2**) or in the dispersed state by DLS ( $170 \text{ \AA}$ ).

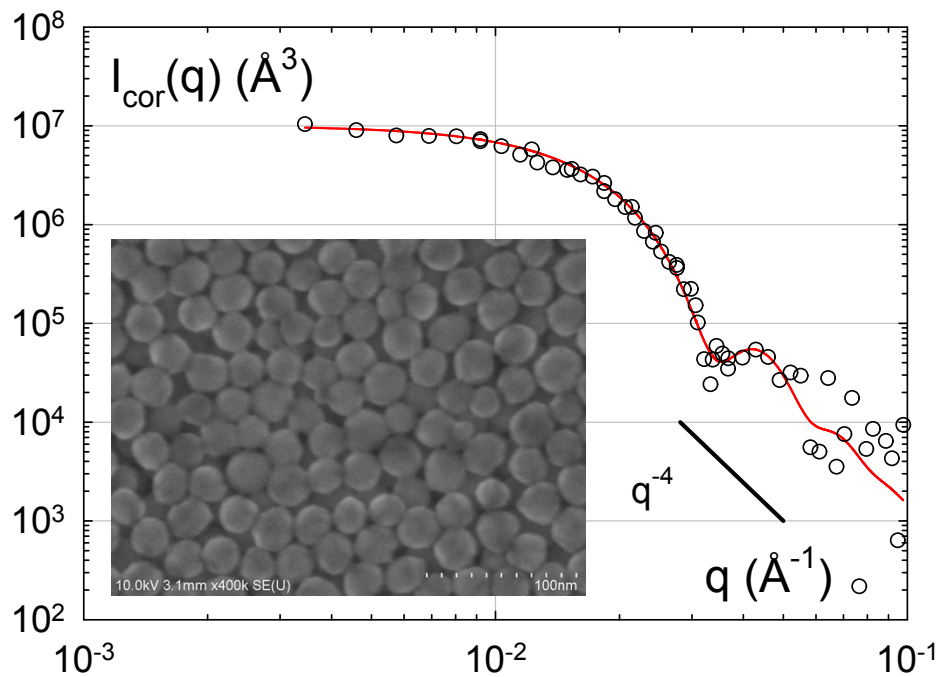


**Figure S2.** Characterization of silica nanoparticles Ludox TM50 by SANS with a double logarithmic plot of the reduced scattering intensity (⊙) obtained from a dilute dispersion of silica nanoparticles ( $C = 1 \text{ wt}\%$ ); the corresponding fit, based on a polydisperse sphere model ( $R_f = 132 \text{ \AA}$  and  $\sigma = 15 \text{ \AA}$ ), is indicated in solid line. The SEM image of silica nanoparticles is given in the inset ( $R_f = 140\text{-}150 \text{ \AA}$ ).

These results also agree with numerous characterization reported on Ludox TM50 in the literature<sup>[1-3]</sup>. As discussed by Orts-Gill and co-workers, which obtained similar values by SAXS, TEM and DLS, the hydrodynamic radius obtained by DLS is generally overestimated in dilute solution due i) to larger objects that contribute to higher intensity and ii) to the increasing particles repulsions observed by dilution<sup>[3]</sup>.

### SANS fitting for concentrated dispersions

In order to model the scattering behaviour of silica dispersions and hybrid hydrogels with a minimum number of adjustable parameters, a hard sphere potential between particles has been assumed. Considering the Percus-Yevick approximation of the Ornstein-Zernike equation, the structure factor for hard spheres can be calculated using the following set of equations:

$$S(q) = \frac{1}{1 + \frac{24\phi_{HS} G(2qR_{HS})}{2qR_{HS}}} \quad \{S1\}$$

with  $R_{HS}$  the radius of hard spheres with volume fraction  $\phi_{HS}$ , and  $G$  a trigonometric function depending on  $q$ ,  $R_{HS}$  and  $\phi_{HS}$  as follows:

$$G(x) = \alpha \frac{(\sin x - x \cos x)}{x^2} + \beta \frac{2x \sin x + (2 - x^2) \cos x - 2}{x^3} + \gamma \frac{\{x^4 \cos x + 4[(3x^2 - 6) \cos x + (x^3 - 6x) \sin x + 6]\}}{x^5} \quad \{S2\}$$

$$\text{with } \alpha = \frac{(1 + 2\phi_{HS})^2}{(1 - \phi_{HS})^4} \quad \beta = -6\phi_{HS} \frac{(1 + (\phi_{HS}/2))^2}{(1 - \phi_{HS})^4} \quad \gamma = \frac{(\phi_{HS}/2)(1 + 2\phi_{HS})^2}{(1 - \phi_{HS})^4} \quad \{S3\}$$

Working with absolute scattering intensities and known formulation parameters like the volume fraction of silica particles ( $\phi_f$ ) and the nature of the diluent, it is possible to fit the experimental data according to equation {8} by using a simple set of unequivocal variables:

$R$ ,  $\sigma$  and  $R_{HS}$ ;  $\phi_{HS}$  being given by  $\phi_{HS} = \phi_f (R_{HS}/R)^3$ .

An example is given in Figure S3.

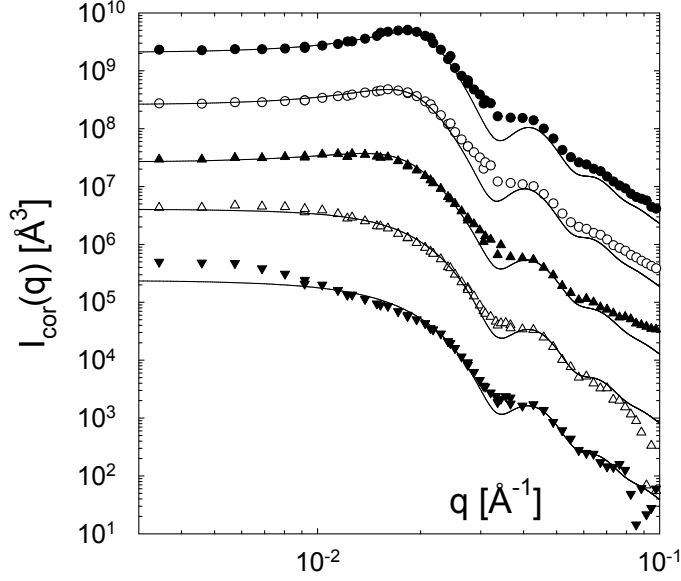


**Figure S3**

Double logarithmic plots of the normalized scattered intensity of PDMA/silica hydrogels (SPx\_PW0.14\_R0.1) prepared in solvent p (silica scattering) with different amount of silica: experimental data for SP0.5 ( $\square$ ), SP1 ( $\circ$ ), SP2 ( $\blacksquare$ ), SP3.5 ( $\odot$ ), SP4.8 ( $\otimes$ ) and model fitting. The curves are shifted from one to another by a factor 10; the bottom one ( $\square$ ) being the reference position.

### Analysis of the corona

Working in solvent f, the filler and the solvent have the same scattering length densities ( $\rho_s = \rho_f$ ) and the situation is similar to a PDMA hydrogel with solvent holes replacing the silica nanoparticles. In this case, we can consider a 3-phase model with: 1) the filler (index  $f$ ), 2) the adsorbed polymer layer at the interface (index  $l$ ) and 3) the PDMA matrix which does not interact directly with the particles (index  $m$ ).

In order to take into account this situation we have used the form factor describing the scattering of the hard sphere interface between the core and the corona (adsorbed polymer layer) and between the corona and the surrounding polymer matrix. The scattering amplitude of the core-shell particle is given by<sup>[4]</sup>:

$$A(q) = V_l (\rho_l - \rho_m) F(q, R_l) + V_f (\rho_f - \rho_l) F(q, R_f) \quad \{S4\}$$

$$\text{or } A(q) = (\rho_p - \rho_s) \{ (\phi_l - \phi_m) V_l F(q, R_l) - \phi_l V_f F(q, R_f) \} \quad \{S5\}$$

with  $\phi_l$  and  $\phi_m$  the volume fraction of polymer in the layer and out of the layer,  $F(q, R_i)$  the scattering amplitude of spheres of radius  $R_i$  defined by {Eq.10} in the manuscript,  $V_i = 4\pi R_i^3/3$  the volume of spheres with  $R_i = R_f + t$  where  $t$  is the thickness of the adsorbed polymer layer (see **Figure S4a**).

The impact of the polymer layer on the amplitude of the form factor is emphasized in **Figure S4b** where the thickness and/or the concentration of polymer have been varied.

As we can see, these modifications involve dramatic changes of scattering patterns due to i) large variations of the scattering volume ( $\{A(q)\}^2 = \{V_l(\rho_l - \rho_m) + V_f(\rho_f - \rho_l)\}^2$ ) as a function of the characteristics of the polymer layer (thickness and concentration) and ii) interferences between the core and the shell that give rise to additional oscillations in the scattering spectrum.

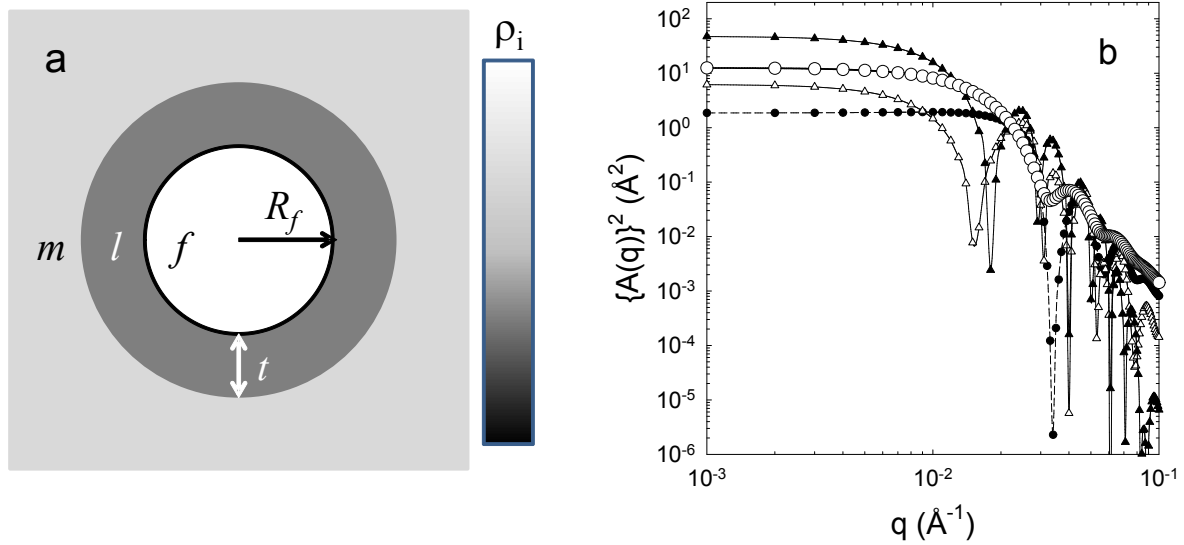


**Figure S4. (a)** Schematic representation of the structure of hybrid network with the silica core (index  $f$ ), the adsorbed polymer layer at the interface (index  $l$ ) and the polymer matrix (index  $m$ ). The grey scale is used to qualitatively picture the level of scattering length densities in the different domains. **(b)** Variation of the square of the scattering amplitude of core-shell particles for various concentration and thickness of the polymer layer ( $R_f = 135 \text{ \AA}$  and  $\sigma = 15$ ):  $t=0 \text{ \AA}$  with  $\phi_l=\phi_p=0.124$  ( $\odot$ );  $t=20 \text{ \AA}$  with  $\phi_l=0.25$  and  $\phi_p=0.116$  ( $\varepsilon$ );  $t=20 \text{ \AA}$  and  $\phi_l=0.50$  and  $\phi_p=0.101$  ( $\square$ );  $t=30 \text{ \AA}$  and  $\phi_l=0.50$  and  $\phi_p=0.070$  ( $\blacksquare$ ).

## 2D SANS

Under uniaxial stretching, an anisotropic scattering pattern is observed for SP2\_PW0.14\_R0.1 hybrid hydrogel. As shown in **Figure S5**, the double wing patterns is preserved at  $\varepsilon = 100\%$  as the volume fraction of silica particles is about two times less compared to SP5 formulation. Nevertheless a four spot pattern is obtained at higher deformation ( $\varepsilon = 370\%$ ); *i.e.* well above the critical value roughly calculated from a simple cubic lattice arrangement:  $\varepsilon_{cr} \cong 200\%$ . We can also notice that when the sample is maintained under high deformation ( $\varepsilon = 370\%$ )

during a long period (10 hours) there is mainly no change in the scattering pattern of the sample and consequently in the distribution of silica particles under large strain.

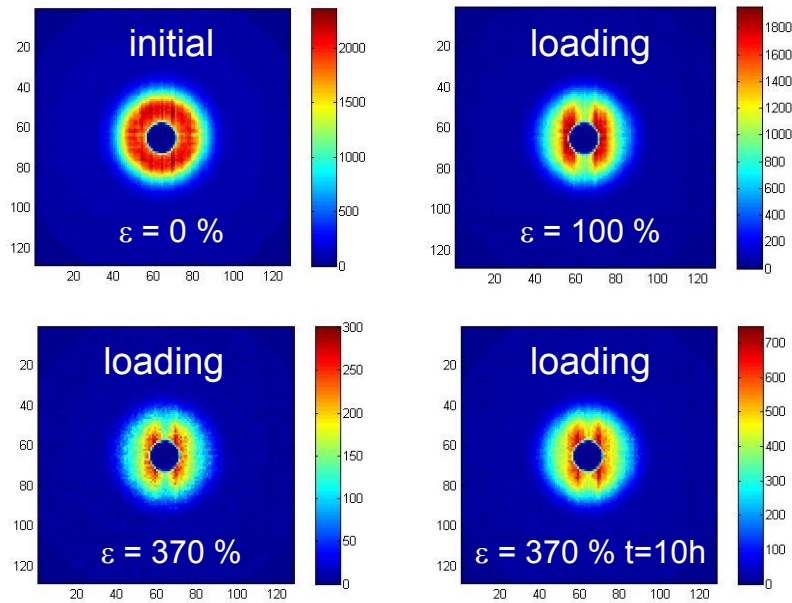


**Figure S5:** 2D-SANS images of SP2\_PW0.14\_R0.1 hybrid hydrogel. Top left: unstrained sample ( $\varepsilon=0\%$ ); top right ( $\varepsilon=100\%$ ); bottom left ( $\varepsilon=370\%$ ); bottom right ( $\varepsilon=370\%$ ) after 10 hours loading at this strain.

When stretched at relatively low deformation ( $\varepsilon = 16\%$ ), the SP5\_PW0.14\_R1 hydrogel fully recovered its isotropic behaviour after unloading (**Figure S6**).

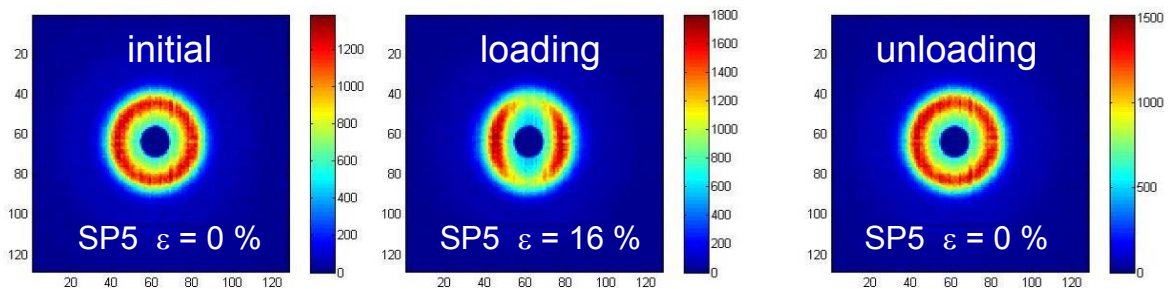


**Figure S6:** 2D-SANS patterns of SP5\_PW0.14\_R1 hybrid hydrogel before loading (left;  $\varepsilon=0\%$ ), under loading (middle;  $\varepsilon=16\%$ ) and after unloading (right;  $\varepsilon=0\%$ ). On the other hand, when the sample SP5\_PW0.14\_R0.1 is stretched well above its critical condition ( $\varepsilon = 200\%$ ) during half an hour and then unloaded back to  $\varepsilon = 45\%$ , the recovery is not complete and the four-spot pattern remains observable even after 3 hours (**Figure S7**).

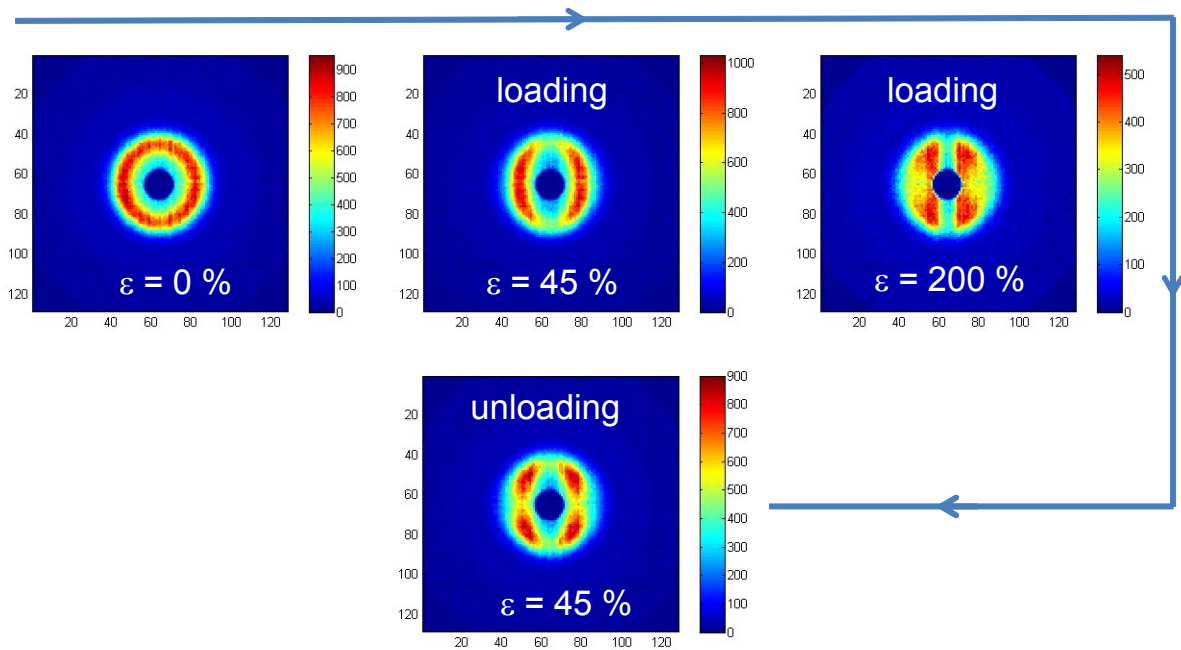


**Figure S7:** 2D-SANS patterns of SP5\_PW0.14\_R0.1 hybrid hydrogel. Top left: unstrained sample ( $\varepsilon=0\%$ ); top middle and top right: loading at  $\varepsilon=45\%$  and then  $200\%$ ; bottom: unloading from  $\varepsilon=200\%$  to  $\varepsilon=45\%$ .

### Reference

- [1] V. Goertz, N. Dingemouts, H. Nirschl, *Part. Part. Syst. Charact.*, 2009, **26**, 17-24.
- [2] N. Hould, R. Lobo, N. Wagner, *Part. Part. Syst. Charact.*, 2010, **27**, 89-99.
- [3] G. Orts-Gil, K. Natte, D. Drescher, H. Bresch, A. Manton, J. Kneipp, W. Osterle, *J. Nanopart. Res.*, 2011, **13**, 1593-1604.
- [4] Suzuki, T.; Endo, H.; Osaka, N.; Shibayama, M. *Langmuir* **2009**, *25*, 8824–8832.